J. Fluid Mech. (1989), *vol.* 204, *pp.* 563–579
Printed in Great Britain

The superharmonic instability of Stokes waves in deep water

By W. J. JILLIANS†
Department of Civil Engineering, University of Delaware, Newark, DE 19716, USA

(Received 19 April 1988 and in revised form 22 November 1988)

The method of Tanaka (1983) is used to solve the eigenvalue problem determining the form of the first superharmonic instability of periodic Stokes waves. Comparisons are made with other approaches to this problem and a discussion of the advantages of Tanaka's method is given. The accurately resolved eigenfunction solution is then taken as the initial state for commencing the computational time-stepping method of Dold & Peregrine (1985), by which we investigate the full nonlinear development of the growing and decaying modes of this instability. It is observed that all unstable modes develop to breaking in the periodic regime and this result is compared and contrasted with the solitary wave case.

1. Introduction

Since Tanaka (1983) published his results for the form of the first superharmonic instability of periodic two-dimensional Stokes waves in deep water – a problem first considered by Longuet-Higgins (1978*a*) – a considerable debate has taken place concerning the location of instability onset measured along the wave height parameter scale. The disagreement grew from Tanaka's finding that the first superharmonic instability mode passed through the energy maximum at the same wave height that it changes from stable to unstable propagation. This seemed to contradict water wave stability theory, as it was then understood, which predicted that this mode would become unstable at the phase speed maximum, otherwise bifurcation to new wave forms would become apparent.

The problem has now been fully resolved and thanks to the analytical work of Longuet-Higgins (1984) and Saffman (1985) we now realize that the only bifurcation to occur at the maximum energy non-limit point is the trivial one of a pure phase shift and so we do not expect the appearance of new waves, in keeping with the uniqueness argument of Garabedian (1965). Thus the eigensolution for the perturbation profile of the first superharmonic instability changes with increase in wave height toward the form of the pure phase shift eigensolution which it comes to resemble exactly at the point of stability exchange. Numerical evidence for this is provided by Tanaka (1985) and an analytic formalism which uses Hamiltonian representation is given by Saffman (1985).

Tanaka (1986) has also studied the linear stability of the solitary wave and found a related zero exchange of stability at the energy maximum of the wave steepness. When this profile is used as the initial condition for a numerical time-stepping scheme it is found that the more slowly growing unstable mode does not necessarily initiate wave breaking. Instead the wave is continuously deformed so that it

† Present address: Department of Aerospace Engineering, University of Southern California, Los Angeles CA 90089, USA.

approaches the form of a stable wave of lower amplitude but closely conserved energy, sending out trailing and radiated waves so that mass and momentum are conserved. Full details of this work are given in Tanaka *et al.* (1987).

The question of the behaviour of periodic Stokes waves under these conditions has no obvious answer since any radiated and trailing waves emitted will not be dispersed to infinity but will be contained to interact further with the basic wave. The time evolution of this instability is thus an open question which we seek to address here.

In §2 we discuss the details of various methods which can be employed to solve both the steady wave and the normal mode time-dependent perturbation problems. Section 3 describes the inverse plane methods and results obtained by normal-mode analysis and we consider the form of the eigenvalues and the perturbation profiles produced by the eigenvectors. Employing the time-stepping scheme of Dold & Peregrine (1985) in §4 we investigate the behaviour of both the faster and slower growing instabilities together with the decaying modes. A discussion of these results and a comparison with the behaviour of the solitary wave are given in §5.

2. Discussion of inverse plane methods

To solve the first-order eigenvalue problem derived from the normal-mode time perturbation of the kinematic and dynamic boundary conditions which determine the behaviour of a free surface we employed two currently available methods. Both are hybrids of the series approach first used by Stokes (1880) in which the physical coordinates (x, y) are represented as Fourier series of the velocity potential ϕ and stream function ψ. The advantage with this approach is that the free surface can be more easily represented as the streamline $\psi = 0$ in the complex potential χ (or inverse) plane than as an unknown function of displacement in the physical plane.

First we consider the problem of steady Stokes waves. The method derived by Longuet-Higgins (1986) incorporates previous work first investigated by Longuet-Higgins (1978*b*) where the Stokes coefficients are evaluated by solving the quadratic relations between them. Tanaka (1983) used the Nekrasov transformation to map the inverse plane into a unit circle. He then concentrated numerical emphasis on the crest region of the wave using a further conformal mapping which compresses computational grid points together there.

In denoting a wave height parameter, Longuet-Higgins uses wave steepness ak which, for a wavelength 2π with normalized wavenumber, will be equivalent to half the vertical difference between the wave crest and trough displacements. Tanaka uses a less easily physically comprehensible parameter ω, where

$$w = 1 - \frac{q_{\text{crest}}}{q_{\text{trough}}} \tag{1}$$

for particle velocity q in the rest frame, which has $\omega = 0$ for infinitesimal waves and $\omega = 1$ for the steepest wave. Both notations will be used here.

In figure 1 we show a plot of x – the horizontal coordinate of displacement – against velocity potential over phase speed, ϕ/c, in a frame of reference moving with the phase speed so that the unperturbed steady free surface is fixed. We note that for steep waves the form of this curve changes in the region of the crest (at the origin) as we increase the wave height parameter toward the maximum 120° crest wave.

Physical plane methods, such as Rienecker & Fenton (1981), in which ϕ/c is considered as a Fourier expansion in x will accurately describe the crest region –

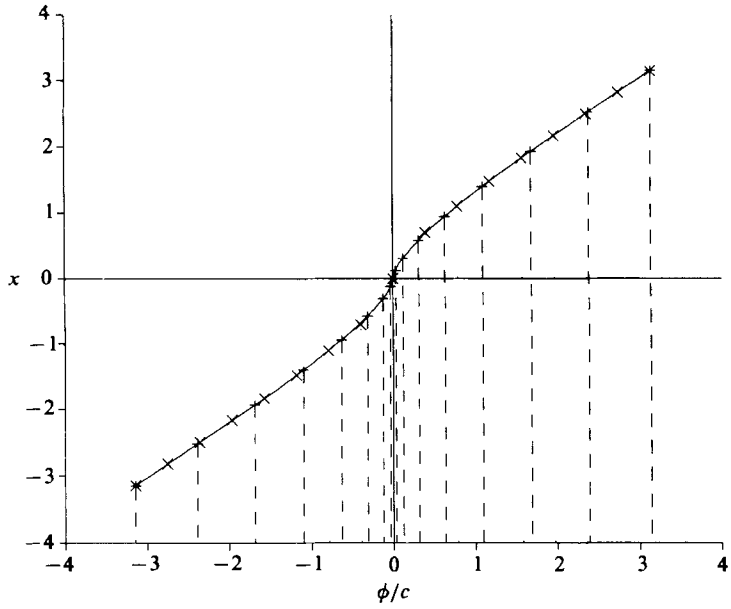

FIGURE 1. Plot of x against ϕ/c for the steady nonlinear periodic wave $\omega = 0.82$ ($ak = 0.4302$). The wave crest is at the origin and the troughs are on either far side. The projection is marked by lines from the curve to the ϕ/c-axis. The two methods have point annotations and projections in the form: Tanaka (+, dashed), Longuet-Higgins (×, dotted).

however, the discontinuous first derivative due to the 120° angle will greatly hinder the convergence of the method for steep waves, particularly since it requires more computational variables. Thus we use an inverse plane method as described earlier.

The problem with the representation of Longuet-Higgins will be that of accurately resolving the free-surface curvature at the crest. This difficulty will not be experienced by Tanaka's method since computational points are concentrated here at the expense of the trough region which can be seen to change little with increasing wave height and so will cause no essential loss of resolution to detract from the method. It will be observed later that for very steep waves the form of the normal-mode perturbation components are most pronounced in the region of the wave crest and become small upon moving toward the wave trough. A computational-grid distribution with emphasis upon the crest is required for good resolution and Tanaka's method has this advantage.

3. Method and results of normal-mode analysis

The complete first-order problem involves the solution of the time-dependent boundary conditions for an incompressible, inviscid, irrotational fluid flow in deep water governed by Laplace's equation, where we work in the reference frame of §2. Particular emphasis is given to Tanaka's method in the following exposition. The boundary conditions are given by

$$\phi_t + \tfrac{1}{2}(\nabla\phi)^2 + \eta = \text{constant}, \tag{2}$$

$$\eta_t + \phi_x \eta_x = \phi_y, \tag{3}$$

for the dynamic and kinematic equations respectively, which must both be solved on the perturbed free surface $y = \eta(x, t)$. Partial derivatives here are denoted by

subscripts of the derivative variable. We expand both solutions into steady and small time-dependent perturbation quantities using

$$\left.\begin{aligned}\eta(x,t) &= H(x)+\tilde{\eta}(x,t),\\ \phi(x,y,t) &= \Phi(x,y)+\tilde{\phi}(x,y,t),\end{aligned}\right\} \tag{4}$$

where $H(x)$ and $\Phi(x,y)$ represent the profile of the free surface and the velocity potential for the steady unperturbed wave respectively. The quantities $\tilde{\eta}$ and $\tilde{\phi}$ are small first-order time-dependent perturbations of these steady functions respectively, whose products and higher powers can be assumed negligible.

To solve the steady wave problem we just need to solve (2) to highest order, neglecting time dependence. We do this using a Fourier sequence of powers of complex coefficients – as outlined in greater detail in Tanaka (1983). The first-order perturbation problem is solved using both (2) and (3) simultaneously and assuming all time dependence is of the form $e^{-i\sigma t}$. We may rewrite this system of equations by expanding the perturbed quantities in a Fourier series which we truncate at $n = N$. Hence we derive $(4N+2)$ homogeneous equations for the coefficients of $\cos n\gamma$ $(n = 0,\ldots,N)$ and $\sin n\gamma$ $(n = 1,\ldots,N)$ from the two nonlinear equations to solve for the unknown eigenvalue and eigenvector $\sigma, \boldsymbol{x}$. The variable γ here is the angular displacement in the unit circle plane upon performing all Tanaka's conformal mappings. By rearranging the positions of elements in our matrices we exploit the fore and aft symmetry of the Stokes wave to write the matrices in the form

$$-i\sigma \boldsymbol{A}\boldsymbol{x} = \boldsymbol{B}\boldsymbol{x}, \tag{5}$$

in which

$$\boldsymbol{A} = \begin{pmatrix} \boldsymbol{A}_1 & \boldsymbol{0} \\ \boldsymbol{0} & \boldsymbol{A}_2 \end{pmatrix}, \quad \boldsymbol{B} = \begin{pmatrix} \boldsymbol{0} & \boldsymbol{B}_1 \\ \boldsymbol{B}_2 & \boldsymbol{0} \end{pmatrix}, \quad \boldsymbol{x} = \begin{pmatrix} \boldsymbol{x}_1 \\ \boldsymbol{x}_2 \end{pmatrix}, \tag{6}$$

where $\boldsymbol{A}_i, \boldsymbol{B}_i\,(i = 1,2)$ are $(2N+1)\times(2N+1)$ square matrices with elements derived from quantities associated with the steady wave problem and $\boldsymbol{0}$ is an identically sized zero matrix. The eigenvalue σ represents the perturbation propagation frequency (if real) or the instability growth rate (if pure imaginary). The eigenvectors $\boldsymbol{x}_1, \boldsymbol{x}_2$ are the in-phase and quadrature Fourier components of the perturbation respectively.

The eigenvalue problem of both author's methods were solved using an inverse iteration technique. In order to ensure convergence for the method we solve the truncated system for sequences of increasing numbers of Fourier modes N, interval ΔN, and estimate the final value, obtained in theory by using infinite modes, employing Richardson's extrapolation formula

$$f_\infty = f_N + \Delta_N \frac{r}{(1-r)} \tag{7}$$

for $\Delta_N = f_N - f_{N-1}, r = \Delta_N/\Delta_{N-1}$ which assumes that each estimate f_N forms a truncated geometric series in powers of r whose limit can be found as $N \to \infty$. We use this procedure to estimate both eigenvalue and individual eigenvector components. The convergents of σ_1^2 and σ_2^2 – the squared eigenfrequency of the pure phase shift and first superharmonic mode respectively – are given in table 1 for some selected values of ω and the estimates produced from the Richardson extrapolation are given in table 2. It is found that the value σ_2^2 passes through zero at the energy maximum $ak = 0.4292$ or $\omega = 0.8135$ in agreement with Longuet-Higgins (1986) and Tanaka (1983).

Slight problems are encountered with convergence in the immediate region of the

N	σ_1^2	Δ	r	σ_2^2	Δ	r
			$\omega = 0.8$			
32	-2.26331×10^{-6}	—	—	0.0148857	—	—
36	-4.85768×10^{-7}	1778	—	0.0148778	−78	—
40	-1.05553×10^{-7}	380	0.214	0.0148776	−16	0.021
44	-2.32243×10^{-8}	82	0.217	0.0148778	17	−1.072
48	-5.17344×10^{-9}	18	0.219	0.0148779	7	0.397
			$\omega = 0.81$			
32	-2.34836×10^{-5}	—	—	0.0040082	—	—
36	-6.25327×10^{-6}	1723	—	0.0039953	−129	—
40	-1.69643×10^{-6}	456	0.264	0.0039920	−32	0.251
44	-4.68691×10^{-7}	123	0.269	0.0039912	−9	0.276
48	-1.31635×10^{-7}	34	0.275	0.0039909	−3	0.283
			$\omega = 0.82$			
48	1.43436×10^{-7}	—	—	−0.0076560	—	—
52	4.21570×10^{-8}	1013	—	−0.0076558	180	—
56	1.25418×10^{-8}	296	0.292	−0.0076558	50	0.279
60	3.77269×10^{-9}	87	0.296	−0.0076558	14	0.291
64	1.14622×10^{-9}	26	0.230	−0.0076558	4	0.294
			$\omega = 0.825$			
36	5.89213×10^{-6}	—	—	−0.0138382	—	—
40	1.84501×10^{-6}	405	—	−0.0138286	956	—
44	5.87515×10^{-7}	126	0.311	−0.0138257	295	0.309
48	1.89998×10^{-7}	40	0.316	−0.0138248	92	0.311
52	6.22993×10^{-8}	13	0.321	−0.0138245	29	0.344

TABLE 1: Convergents to σ_1^2 and σ_2^2 using Tanaka's method

ω	$N_{\max}$	σ_1^2	σ_2^2	σ_2
0.8	48	-6.4226×10^{-10}	0.014878	0.12198
0.81	48	-1.9359×10^{-9}	0.003991	0.06317
0.82	64	9.8220×10^{-12}	−0.007656	$0.08750i$
0.825	52	7.1616×10^{-10}	−0.013824	$0.11758i$

TABLE 2. Estimates of σ_1^2, σ_2^2 and σ_2 using Tanaka's method where $N_{\max}$ is the number of coefficients used in extrapolation

energy maximum since the inverse iteration scheme cannot distinguish the two eigenvectors easily when they are close together. We can overcome this problem by calculating all eigenvalues of the system to some order precisely using a separate scheme and then starting the inverse interaction scheme with this exact value to guarantee convergence. The results show that we can expect the eigenvectors for the pure phase shift mode and first superharmonic instability to become identical as $\omega \to 0.8135$, as Tanaka first found.

In calculating the eigenvalues and eigenvectors, the method of Longuet-Higgins gave much larger values of r in equation (7) for both eigenvalues and the moderately steep wave eigenvector components, implying slower convergence. The extrapolated eigenvalues were very close to those of table 2; however problems were encountered with eigenvector convergence which became worse with increasing wave steepness. For waves in the vicinity of the energy maximum, 144 Fourier coefficients were calculated requiring 900 CPU seconds of computation on an IBM 3081 system. It was

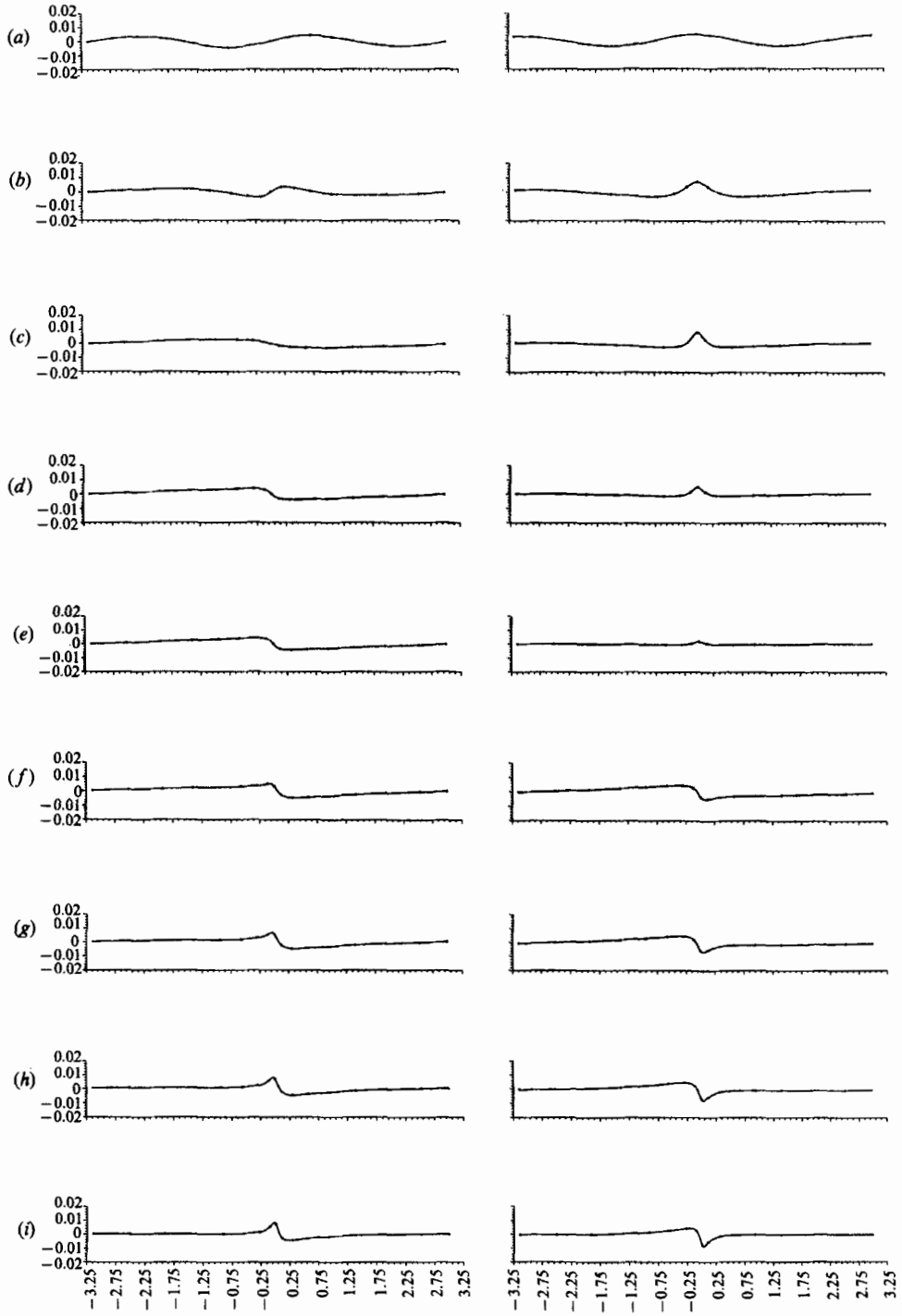

FIGURE 2. Plots of the quadrature (left) and in-phase (right) components for different wave heights in stable equilibrium for σ_2: (*a*) $\omega = 0.2$, (*b*) 0.7, (*c*) 0.8, (*d*) 0.81 (*e*) 0.813. Also in unstable equilibrium with the decaying mode (left) and growing mode (right): (*f*) $\omega = 0.815$, (*g*) 0.82, (*h*) 0.83, (*i*) 0.85. The perturbation components have $\epsilon = 0.01$.

found that there was a 0.035 radian angular displacement margin of error in N-dimensional vector space between subsequent calculations ($\Delta N = 12$) of the perturbation vector of the Fourier coefficients. This was working at the limit of the machines memory resources. We should compare this to the maximum of 64 Fourier coefficients needed by Tanaka's method which require 300 CPU seconds on an identical machine to calculate to within a 3.5×10^{-6} radian angular displacement margin of error between subsequent calculations.

With the values of the eigenvectors found using Tanaka's method we can calculate the form of the perturbed profiles to first order in the linearized perturbation quantities. Some care must be taken over the signs of the velocity potential and displacement perturbations, $\tilde{\phi}, \tilde{\eta}$, which are dependent upon the direction of propagation of the basic wave.

The plots of the σ_2 mode perturbations are given in figure 2 for both the in-phase and quadrature components of the propagating disturbance and the growing and decaying components once the instability becomes effective. For the smallest amplitudes in stable equilibrium (figure 2*a*) both disturbance components resemble two sinusoidal waves with wavelength half that of the basic wave. As the wave steepness increases we still have what appears to be two sinusoidal components but their effect has become very localized in the region of the crest (figure 2*b*). By $\omega = 0.8$ ($ak = 0.426$, figure 2*c*) the quadrature component seems to have lost all the half-wavelength structure and more closely resembles the full-wavelength modulation of the σ_1 mode. At $\omega = 0.81$ ($ak = 0.4286$, figure 2*d*) the in-phase component is obviously decaying and the quadrature component looks even more like the pure phase shift modulation. This process continues until we have almost exact resemblance just before the energy maximum is reached with $\omega = 0.813$ ($ak = 0.4291$, figure 2*e*). After we pass through stability exchange we must consider the decaying and growing components of the wave, which at $\omega = 0.815$ ($ak = 0.4294$, figure 2*f*) look almost identical, with the only difference between them being either an addition or subtraction of what was the calculated in-phase-component – a still very small value as it slowly grows from zero at the point of stability exchange. As the wave height is increased further this value continues growing and the difference between decaying and growing modes becomes more evident with both looking progressively less like the form of the pure phase shift. As the wave height is increased toward $\omega = 0.85$ ($ak = 0.4344$, figure 2*i*) the decaying mode perturbation develops a local maximum on the rear face of the crest, which has decreasing radius of curvature and is becoming a sharp angular feature. Similarly the growing mode perturbation develops a local minimum on the forward face of the crest which becomes more pronounced as wave height is increased. It may be feasible to draw some comparisons between these features and the increase of growth/decay rates of the perturbations, and in particular we shall observe in §4 the growing mode perturbation feature to always be present in time-stepped profiles which tend toward breaking.

4. Results for time-stepping

The profiles derived above and shown in figure 2(*g*) for the $\omega = 0.82$ ($ak = 0.4302$) unstable wave perturbation, calculated using Tanaka's method, are now used as the initial data for a discretized time-stepping method to observe the nonlinear evolution of the unstable disturbances. The environment of this scheme is such that $g = 1$ and the wavelength is 2π considered in the range $[0, 2\pi]$. Periodic boundary conditions

apply so that any marked free-surface particle moving out of range at one end will rejoin it at the other.

One feature of this Dold & Peregrine (1985) time-stepping method which we use is that the most accurate results for long-time calculations are given if the particle spacing is proportional to the particle velocity in the stationary reference frame of the steady wave. To achieve the required point redistribution accurately an 11-point interpolation formula is used together with an iteration procedure to calculate optimal values for the horizontal and vertical displacements of the wave and for the velocity potential at each interpolated point. We test our redistributed profile of the steady wave using Bernoulli's equation to calculate the error introduced by the interpolation method. We find the maximum error in the pressure over the redistributed wave profile as a percentage of the constant value to be $5 \times 10^{-11}\%$ which is no different to that calculated from the uninterpolated wave data using Tanaka's method.

As a measure of displacement change we introduce the growth function $R(t)$ which we calculate as

$$R^2(t) = \frac{\int_0^{2\pi} h^2(x,t)\,\mathrm{d}x}{\int_0^{2\pi} h^2(x,0)\,\mathrm{d}x}, \tag{8}$$

where $h(x,t)$ is the vertical disturbance from the unperturbed Stokes wave found using the 11-point interpolation formula on the profile calculated by time-stepping after a certain time t.

We can attempt to recover linear stability growth, or a close resemblance to it for small but finite ϵ, using an initial disturbance in the time-stepping scheme that is slightly larger than the errors introduced by the scheme itself. First we have to test for the error magnitudes involved when operating the scheme with a steady steep Stokes wave ($\omega = 0.82$) and no perturbation. Thus the value of h obtained will be a measure of scheme-dependent error. It is found that the vertical disturbance h is negligible for the time that the scheme operates. More precisely the maximum computed value of $\int_0^{2\pi} h^2\,\mathrm{d}x$ for $0 \leqslant t \leqslant 12$ was found to be 10^{-9}. These results act as a control for the following work.

We note here the results of some of the time-stepping calculations to recover linear stability growth using the method of Longuet-Higgins. Tests of the steady wave calculated using the quadratic Stokes coefficient relations found an inherent instability of the wave at the crest which grew so that profile instability was induced. This was obviously a result of poor resolution of the wave crest using this method and implied that this artifact would have become dominant in any attempt to calculate the nonlinear development of the first-order perturbation. To attempt to resolve this we tried to find the solution by combining Tanaka's steady wave method and then calculating the perturbation disturbance using Longuet-Higgins (1986). When this was implemented it was found that linear stability could not be recovered with the growing solutions initially increasing much faster than linear growth and then settling down to a growth between the expected linear rate and more than twice its value – leading quickly to wave breaking. When these results were found it was decided to try to obtain the solutions uniquely using Tanaka's complete method, with much more satisfying consequences. We describe the results thus obtained under separate headings for the two unstable cases of the growing and decaying modes.

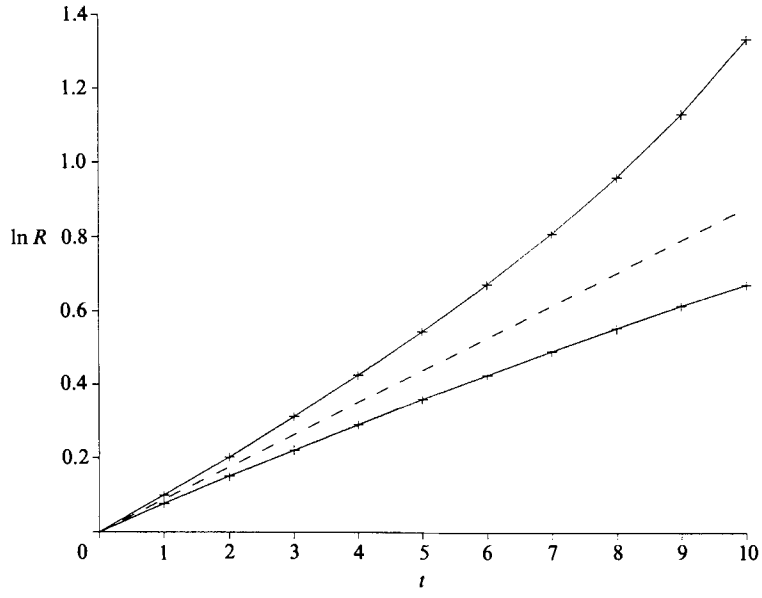

FIGURE 3. Growth of the $\omega = 0.82$ unstable wave modulations with perturbation magnitude $|\epsilon| = 0.01$ plotting $\ln R$ against time. The predicted linear growth is shown by the dashed line. The faster growing solution has $\epsilon = 0.01$ and the slower growth has $\epsilon = -0.01$.

4.1. *The growing modes*

For a large initial perturbation $\epsilon = 0.01$ there is initially a very slight divergence from linear stability with time which increases as nonlinear effects begin to exert their influence, as can be seen in figure 3 which shows the exponential growth rate $\ln R$ with time. Both solutions have significantly diverged by $t = 1.0$ and we go on to describe their time evolution separately, first for the quickly growing ($\epsilon = 0.01$) and then the slowly growing mode ($\epsilon = -0.01$).

Plots of the quickly growing perturbed wave developing under the time-stepping are portrayed in figure 4, together with a plot of the function $h(x, t)$ at given times, with vertical scale expansion by a factor of 12 to better reveal the nature of the disturbance. In this figure every fourth fluid particle in the discretization of the free surface is marked. We see that after the initial growth of the perturbation, the nonlinear effects act to deepen the trough of the perturbation to a more accentuated downward curve than the neighbouring perturbation peak. Thus the wave profile itself gradually develops slight asymmetry with the forward wave face steeper than the rear. By $t = 8.63$ the wave seems to be developing a finite-angle crest whose remaining radius of curvature is reduced as the wave propagates. By $t = 10.0$ the radius of curvature in the immediate vicinity of the crest has become very small and from this point a forward-projecting jet is produced which overturns and tends toward breaking which takes place shortly after $t = 10.3$.

After the results of Tanaka *et al.* (1987) for the slowly growing solution of the solitary wave instability, we expect the corresponding periodic wave solution to be highly interesting and exhibit unusual properties. When we time-step this configuration we find that the perturbation initially serves to reduce the overall height of the wave (see figure 5). The perturbation grows with time up until $t = 11.5$ with a smaller radius of curvature on the forward wave face at the perturbation maximum and a more rounded curvature in the minimum. The overall wave height

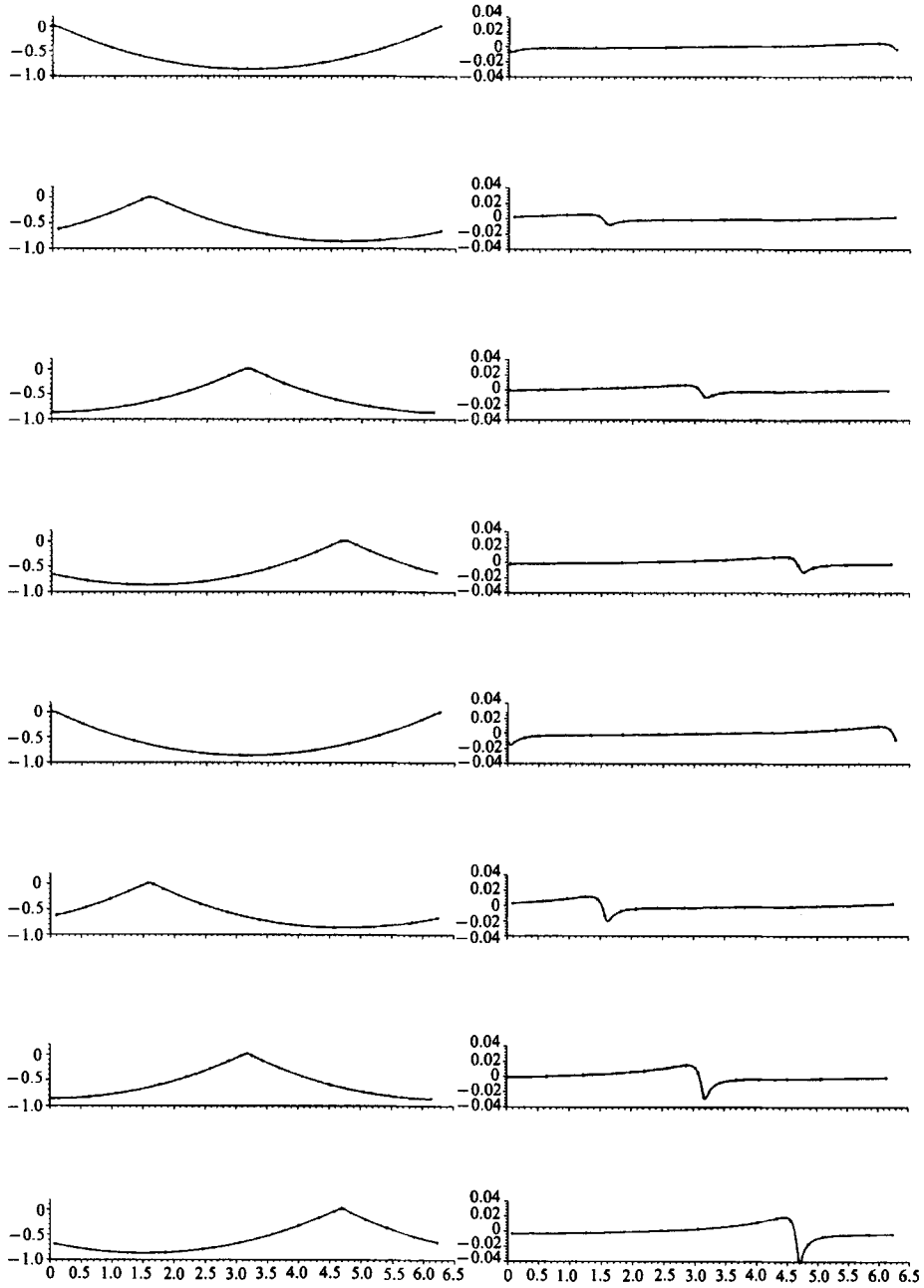

FIGURE 4. The time development of the quickly growing $\omega = 0.82$ wave unstable mode started with $\epsilon = 0.01$. The left-hand diagrams represent the wave profile while the right-hand diagrams are the disturbance $h(x, t)$ from the steady wave profile. The time development is taken from $t = 0$ to $t = 10$ with plots made every quarter-wave period ($t = 1.44$) downwards.

is at its smallest value now. Gradually the sharp perturbation disturbance from the original wave has become spread along the whole wavelength. This bears some resemblance to the production of a linear trailing wave from the basic wave whose amplitude is growing to a maximum, as in the case of the solitary wave.

As time progresses the overall wave height monotonically increases and by $t = 46$

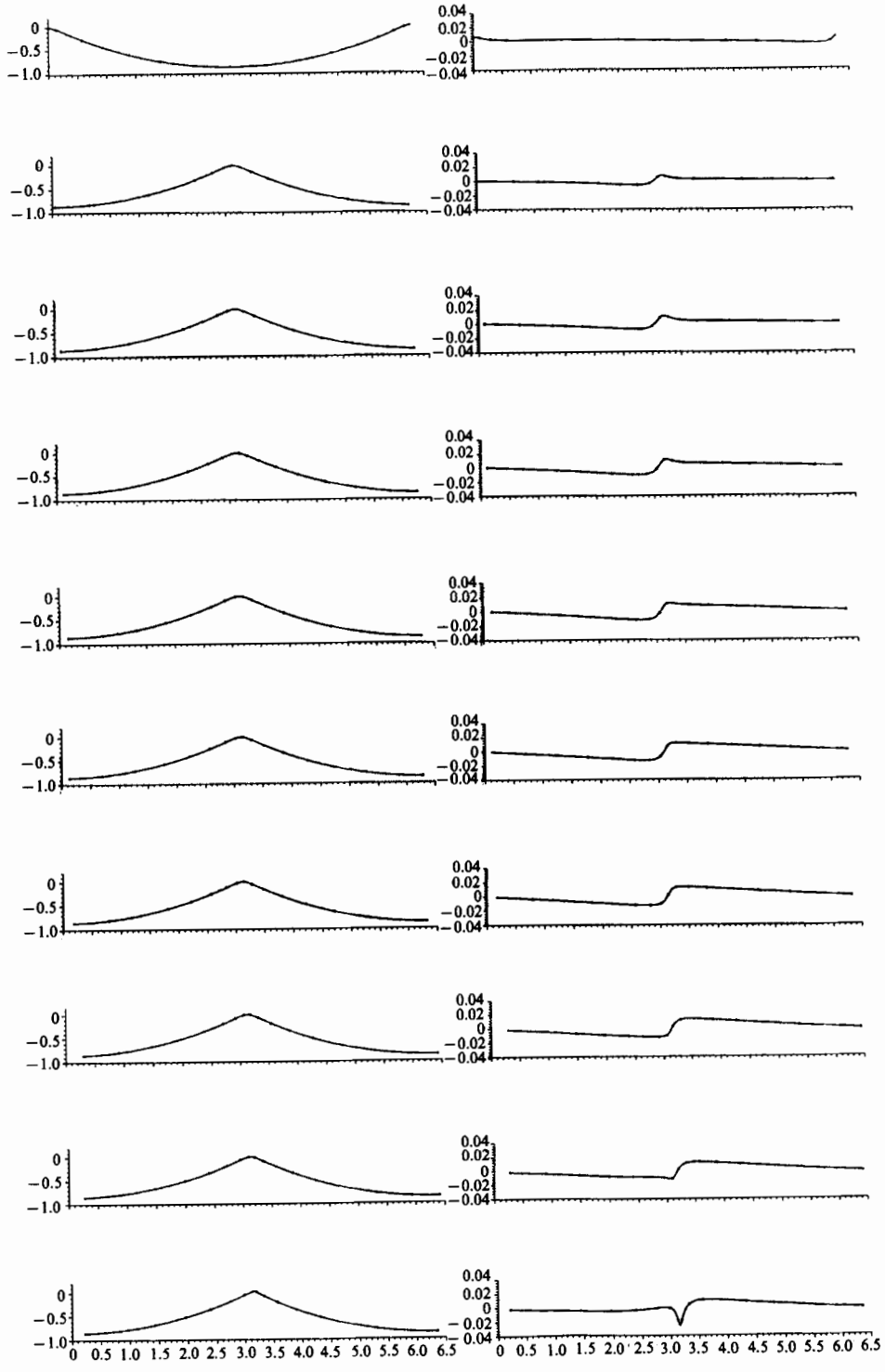

FIGURE 5. The time development of the slowly growing $\omega = 0.82$ wave unstable mode started with $\epsilon = -0.01$ laid out as in figure 4. The time development is taken from $t = 0$ to $t = 48.88$ with the second plot taken after a half-wave period and subsequent plots made every wave period ($t = 5.75$) downwards.

a sharp curvature has appeared in the perturbation minimum, which has moved to the forward face of the wave as a result of the reduction in amplitude of the basic wave and a subsequent reduction in its phase speed. This perturbation minimum deepens and becomes more sharply accented in the manner of the faster growing solution and a new local maximum in the perturbation starts to grow on the rear face of the wave. By $t = 50$ the wave has exceeded the maximum height for stable propagation and breaking is likely to occur. The wave overturns and tends toward breaking, which happens at some time slightly before $t = 50.3$.

4.2. *The decaying modes*

The growth rates for the decaying modes are shown in figure 6 for $|\epsilon| = 0.01$. Both are seen to decay initially at close to the negative linear growth rate, but one solution decays slightly faster than the other, so we denote these the rapidly decaying ($\epsilon = -0.01$) and slowly decaying ($\epsilon = 0.01$) modes, regardless of the later evolution.

For the rapidly decaying solution after initial linear decay and nonlinear effects, which cause the growth curve to deviate slightly from the linear prediction, we see that after $t = 7$ a very strong nonlinear reaction begins which stops the perturbation from decreasing further and by $t = 9$ has initiated what appears to be almost linear growth. Inspecting the perturbation-plot development with time in figure 7 we see that the large curvature in the minimum at $t = 0$ remains throughout the motion and that the small radius of curvature maximum on the forward face of the wave is reduced to the benefit of a growing rear-wave-face local maximum. By $t = 8.63$ they are equal and subsequently the rear-face maximum grows, together with the forward-face minimum until overturning and breaking finally occurs at about $t = 18.4$. The form of the perturbation curvature close to the crest when leading up to and during overturning is very similar to that described for the growing modes.

For the slowly decaying solution shown in figure 8 we initially have linear decay and slight nonlinear effects deflecting the result away from the linear stability curve again. At $t = 5.75$ we again experience strong nonlinear effects which reverse the decay process and initiate an almost linear growth slightly larger than the predicted linear value but not as large as the similar nonlinear growth of the rapidly decaying mode. From the perturbation profiles we see that the small radius of curvature of the crest maximum on the rear face is rapidly eliminated by $t = 5.75$, and by $t = 17.26$ a small radius of curvature minimum on the forward wave face has started to grow together with a rear-face perturbation maximum. Again the perturbation approach to breaking is as described in the other three modes, as is the form of the wave profile.

Comparisons between the later growth rates of the decaying modes and those of the growing modes indicate that both decaying solutions appear to be behaving similarly to the quickly growing mode, although there is not a precise correlation. To explain this breaking phenomenon for the decaying modes we can at present only suggest possible, and conflicting, physical and computational reasons for this behaviour.

Physically, for a moderate initial perturbation $|\epsilon| = 0.01$ there will be a finite energy disturbance of the basic wave which cannot decay to zero unless energy conservation be violated. Thus as the wave propagates, the nonlinear effects together with energy conservation must transfer energy into the growing modes, in some manner. Growth to breaking will occur in order to dissipate the excess energy of the wave for recovery of stable propagation. We cannot expect all decaying solutions to tend to disappear completely without some interesting nonlinear effects taking place.

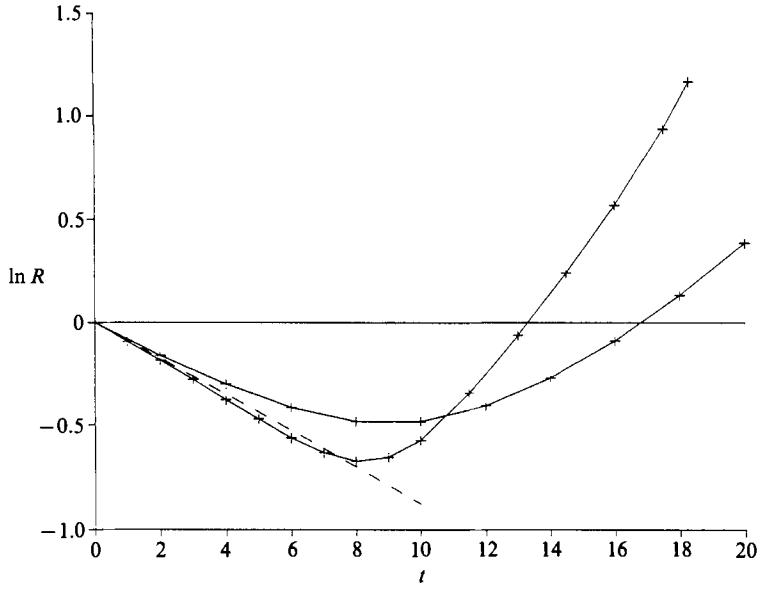

FIGURE 6. Decay and growth of the $\omega = 0.82$ wave decaying modes with perturbation magnitude $|\epsilon| = 0.01$ plotting $\ln R$ against time. The predicted linear decay is shown by the dashed line. The slowly decaying solution has $\epsilon = 0.01$ and the rapid decay has $\epsilon = -0.01$.

Computationally, we must consider stability theory in the vicinity of a stationary point. Because the solution we compute for the decaying modes will always involve a truncation error, we can never find the decay to zero of the perturbation which an ideal decaying mode would experience. Our solution lies close to this ideal decaying mode and approximate linear decay will be experienced initially. However, as we move closer to the stationary point the truncation error will have some small component of a growing mode which will increase exponentially with time. Simultaneously the decaying mode will decrease until the growing mode is dominant and we experience linear growth, as observed at later times in figure 6.

It is not immediately obvious which of these mechanisms will be responsible for this numerically observed phenomenon, which may be caused by either or be due to both. Decaying modes may provide difficult to produce and observe experimentally which seems, with some speculation, to be the only way to fully resolve the physics of this interaction.

5. Discussion

We have examined and employed two approaches to the problem of two-dimensional Stokes wave superharmonic instabilities and both intuitively and in practice we find Tanaka's method of coordinate stretching points about the wave crest to be a technique applicable and accurate almost up to the highest wave. Using this method we have calculated the time evolution of all the growing and decaying components of the instability.

This method is equally reliable for the study of other problems of Stokes wave instabilities. To illustrate we could have used this method to find the *small-scale* superharmonic instability of MacKay & Saffman (1986), which they found using the

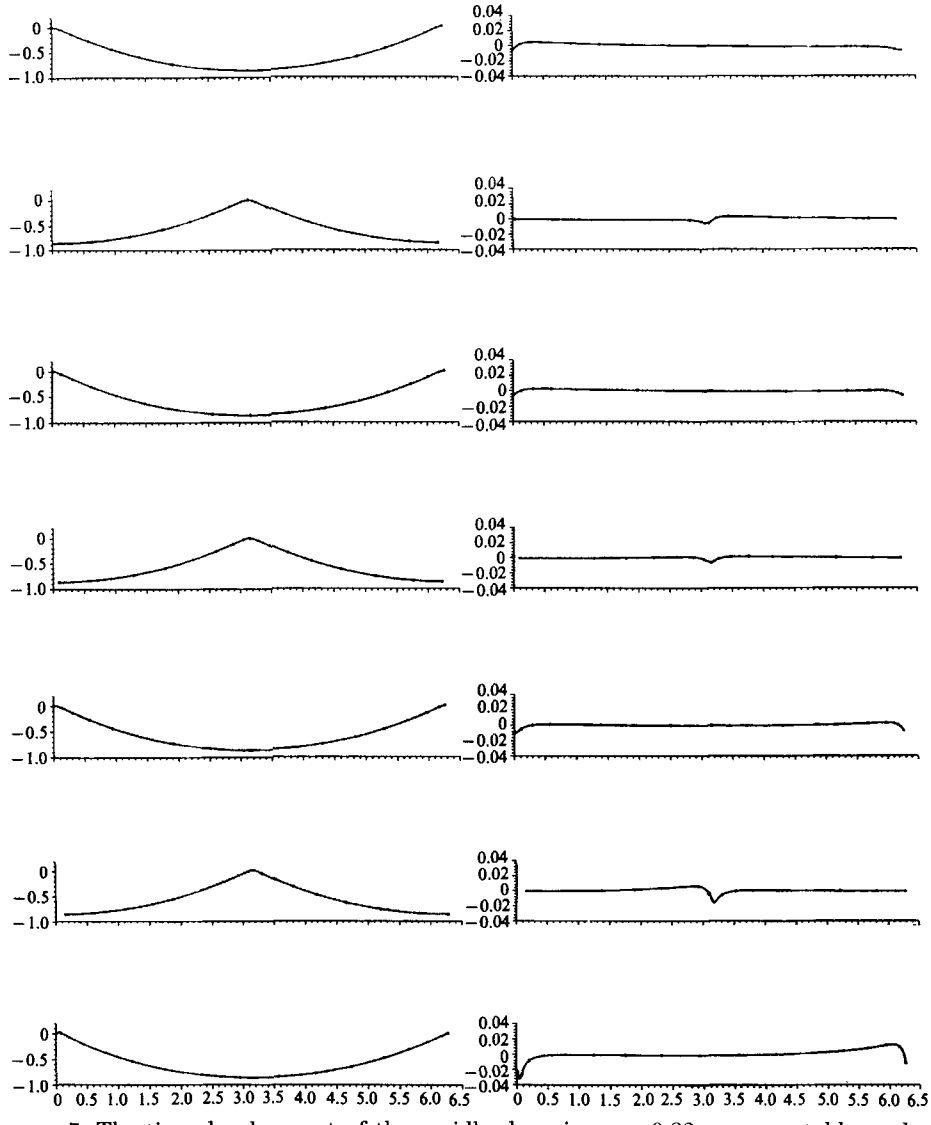

FIGURE 7. The time development of the rapidly decaying $\omega = 0.82$ wave unstable mode started with $\epsilon = -0.01$ laid out as in figure 4. The time development is taken from $t = 0$ to $t = 17.25$ with plots made every half-wave period ($t = 2.875$) downwards.

Hamiltonian representation of Stokes waves employing a method not discussed in any detail here. From our knowledge of that procedure we speculate that Tanaka's method would have given a more computationally economical result.

For the time-stepping results it should be noted that there is great similarity between the breaking process exhibited by all four instability solutions since each is seen to be a local effect at the wave crest with a sharp minimum perturbation on the forward wave face and a more gently curving maximum on the rear face giving slight asymmetry and resulting in the wave breaking in its direction of propagation. This seems to support the contention held by many workers that some examples of breaking are purely local phenomena which, in the case of spilling breakers and more gently plunging breakers, occur independently of the flow in the rest of the wave.

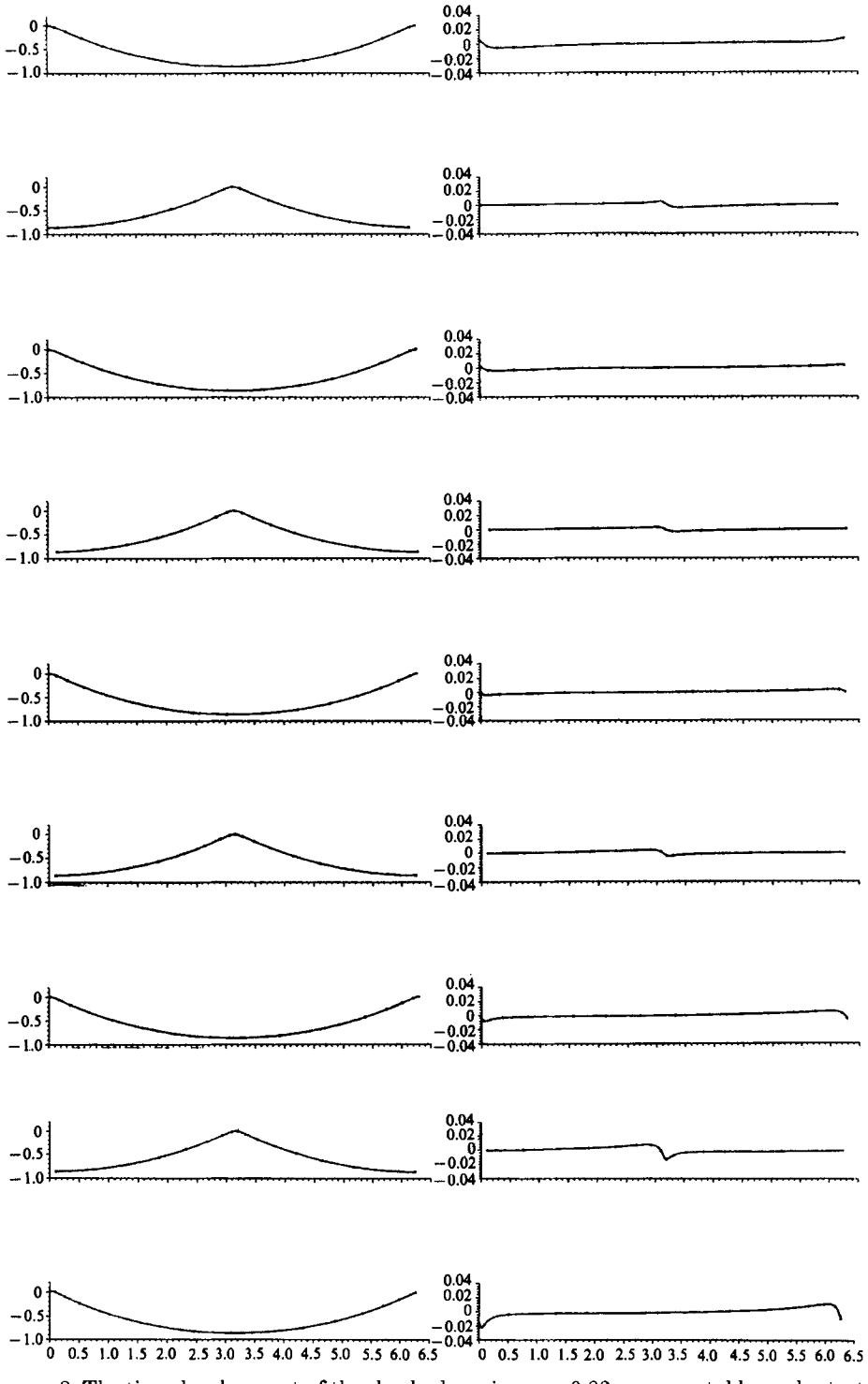

FIGURE 8. The time development of the slowly decaying $\omega = 0.82$ wave unstable mode started with $\epsilon = 0.01$ laid out as in figure 4. The time development is taken from $t = 0$ to $t = 23$ with plots made every half-wave period downwards.

Comparing the slowly growing mode to the case of the solitary wave, it is clear that because we are now working in a periodic environment then if either radiated or trailing waves are emitted by the basic wave to lower its mass and momentum we have little opportunity to resolve and identify them. If produced these waves will move away from the basic wave in their initial stages of development in a form that we are unable to distinguish apart from the basic wave and its time-dependent perturbation component (the long waves emitted by the solitary waves in Tanaka *et al.* are not properly resolved until they move away from regions of large displacement due to the solitary wave). However, in a periodic environment these disturbances will re-encounter the wave as it moves forward and they travel back. They may then proceed to act on the wave in a manner so as to force it to break – but we cannot be sure because the process in this environment will be practically indistinguishable from that of a straightforward 'growth to breaking' mechanism. Further detailed work with the slowly growing perturbation will be necessary before we can be sure of the physical process of breaking. Certainly the concepts of trailing and radiated waves seem inappropriate for serious consideration of periodic wave instabilities.

It would be interesting to compare the decaying modes of the solitary wave instability to see if these all lead to breaking, as we experience here, or whether linear waves are emitted so that mass and momentum are dissipated in that way. Bearing in mind the behaviour of the growing modes, it seems possible that at least one decaying mode will behave in this non-breaking manner.

The author would like to thank his supervisor Professor M. S. Longuet-Higgins for suggesting the problem and acknowledges financial support from the Science and Engineering Research Council and the Royal Society over the period of performing this research. Acknowledgements are due to Drs Tanaka, Dold and Professor Peregrine for permission and help in using their respective computational schemes. I am also extremely grateful to Dr R. A. Dalrymple and to the University of Delaware for providing me with resources to complete this work.

REFERENCES

Dold, J. & Peregrine, D. H. 1985 An efficient boundary-integral method for steep unsteady water waves. In *Numerical Methods for Fluid Dynamics II* (ed. K. W. Morton & M. J. Baines). Clarendon.

Garabedian, P. R. 1965 Surface waves of finite depth. *J. Analyse Math.* **14**, 161–169.

Longuet-Higgins, M. S. 1978*a* The instabilities of gravity waves of finite amplitude in deep water. I Superharmonics. *Proc. R. Soc. Lond.* A **360**, 471–488.

Longuet-Higgins, M. S. 1978*b* Some new relations between Stoke's coefficients in the theory of gravity waves. *J. Maths Applics.* **22**, 261–273.

Longuet-Higgins, M. S. 1984 On the stability of steep gravity waves. *Proc. R. Soc. Lond.* A **396**, 269–280.

Longuet-Higgins, M. S. 1986 Bifurcation and instability in gravity waves. *Proc. R. Soc. Lond.* A **403**, 167–187.

MacKay, R. S. & Saffman, P. G. 1986 Stability of water waves. *Proc. R. Soc. Lond.* A **406**, 115–125.

Rienecker, M. M. & Fenton, J. D. 1981 A Fourier approximation method for steady water waves. *J. Fluid Mech.* **104**, 119–137.

Saffman, P. G. 1985 The superharmonic instability of finite-amplitude water waves. *J. Fluid Mech.* **159**, 169–174.

STOKES, G. G. 1880 Considerations relative to the greatest height of oscillatory irrotational waves which can be propagated without change of form. *Mathematical and Physical Papers*, vol. 1, pp. 225–228. Cambridge University Press.

TANAKA, M. 1983 The stability of steep gravity waves. *J. Phys. Soc. Japan* **52**, 3047–3055.

TANAKA, M. 1985 The stability of steep gravity waves. Part 2. *J. Fluid Mech.* **156**, 281–289.

TANAKA, M. 1986 The stability of solitary waves. *Phys. Fluids* **29**, 650–655.

TANAKA, M., DOLD, J., LEWY, M. & PEREGRINE, D. H. 1987 Instability and breaking of a solitary wave. *J. Fluid Mech.* **185**, 235–248.